Dual-targeted Therapy Based On The Macrophage Niche In Rheumatoid Arthritis

Siyue Tao[1,2], Jian Chen[1,2], Fengdong Zhao[1,2]
1. Department of Orthopaedic Surgery, Sir Run Run Shaw Hospital, Zhejiang University School of Medicine
2. Key Laboratory of Musculoskeletal System Degeneration and Regeneration Translational Research of Zhejiang Province
Address: No. 3, Qingchun Road East, Hangzhou, 310016, P.R.China.
E-mail: 12018284@zju.edu.cn

Disclosures: S. Tao: None. J. Chen: None. F. Zhao: None

INTRODUCTION: Inflammatory infiltration and bone destruction are important pathological features of rheumatoid arthritis (RA), which originate from the disturbed niche of macrophages. Here, we identified a niche-disrupting process in RA: due to overactivation of complement, the barrier function of *VSIg4*$^+$ lining macrophages is disrupted and mediates inflammatory infiltration within the joint, and thereby activating excessive osteoclastogenesis and bone resorption. However, complement antagonists have poor biological applications due to super-physiologic dose requirements and inadequate effects on bone resorption.

METHODS: To investigate the pathogenic mechanisms and targets related to RA, we initially conducted an analysis of single-cell sequencing data from synovial *CD45*$^+$*CD11b*$^+$*Ly6G*$^-$ monocyte-derived macrophages in the dataset GSE134420. This analysis aimed to explore the relationship between complement and the imprinting of macrophages in the joint microenvironment. To address excessive complement activation in RA, we developed a novel recombinant fusion protein, CRIg-CD59, and validated its anti-rheumatic activity in a rat model of antigen-induced arthritis (AIA). Following the identification of limitations such as dose dependency and limited effects on bone resorption of the protein, we further advanced the development of a dual-targeted therapeutic nano-platform based on a metal-organic framework (MOF). This platform enabled bone-targeted delivery of the complement inhibitor CRIg-CD59 and pH-responsive release. The surface mineralization of ZIF8@CRIg-CD59@HA@ZA targeted the acidic microenvironment of RA bone, while the sustained release of CRIg-CD59 could recognize and prevent the formation of membrane attack complexes (MAC) on the surface of healthy cells. Through Micro-CT, histological staining, and immunofluorescence analyses conducted on AIA rats treated with ZIF8@CRIg-CD59@HA@ZA, we verified the anti-RA activity of the dual-targeted nano-platform and its effects on *VSIg4*$^+$ lining macrophages and osteoclasts. Lastly, we focused on the characterization and validation of subpopulation features and proportions of joint macrophages using single-cell sequencing after treatment with ZIF8@CRIg-CD59@HA@ZA in RA.

RESULTS SECTION: GO and KEGG analysis revealed the central role of complement cascade in RA. Cell-specific GO analysis revealed significant enrichment tendencies of osteoclasts, further elucidating the relationship between complement and the imprinting of macrophages in the joint microenvironment: activation of osteoclasts and mediation of bone matrix remodeling. Recombinant protein CRIg-CD59 was constructed using seamless cloning and protein purification techniques. In vitro experiments confirmed the efficient expression of the protein and its anti-complement activity. The therapeutic results in the rat AIA model suggested that high-dose treatment with CRIg-CD59 significantly reduced IL-6 and TNF-α levels in RA but had limited alleviation of bone destruction. Subsequently, we prepared a dual-targeted nanoplatform, ZIF8@CRIg-CD59@HA@ZA, and validated its effective pH-dependent release, complement inhibition activity, bone targeting ability, and RA therapeutic activity through in vitro and in vivo experiments. Animal studies and single-cell sequencing results confirmed that the dual-targeted therapy could effectively suppress complement and osteoclast activation, while reducing M1 macrophages and increasing M2 resident macrophages, thereby improving the macrophage niche for the treatment of RA.

DISCUSSION: Various strategies have been tested in animal models using complement inhibitors, such as soluble CR1 (which inhibits complement activation at the C3 level), recombinant C3a and C5a receptor antagonists, and CD59 (which inhibits MAC formation), with promising results. In preclinical animal models of RA, selective administration of anti-C5 antibodies demonstrated therapeutic potential in preventing or treating arthritis. However, the C5aR inhibitor PMX53 and the anti-IL-6 receptor monoclonal antibody tocilizumab have both been found to be ineffective in treating RA. These observations indicate that additional investigation is required to identify complement as a potential therapeutic target for the treatment of RA. Our study highlights the limitations of single drug components in addressing complex pathological mechanisms of diseases, and suggests that nanoplatforms may not only provide efficient carriers for drug delivery but also offer comprehensive treatment of disease pathology through rational design to compensate for functional deficiencies of drugs. This provides a direction for future research and design of RA treatment strategies.

SIGNIFICANCE/CLINICAL RELEVANCE: This combination therapy is expected to treat RA by reversing the core pathological process, circumventing the pitfalls of traditional therapy.

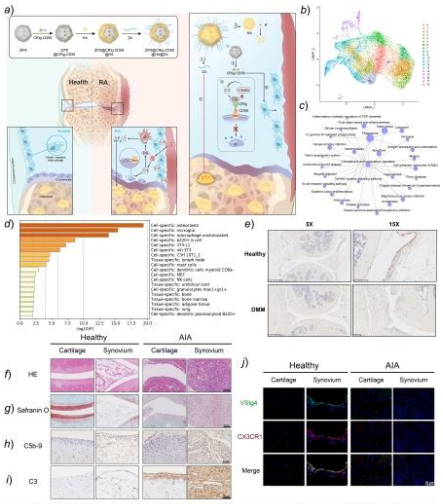

Figure 1. Features of Macrophage Niche in the Pathogenesis of RA. (a) Assembly process and therapeutic mechanism of metal-organic framework-based dual-targeted nanopolymers for the treatment of rheumatoid arthritis. Rheumatoid arthritis is characterized by persistent complement-activating inflammation and osteoclast-activated bone erosion. Disruption of barrier function in *VSIg4*$^+$ lining macrophages is an important feature of RA synovial niche homeostasis.(b) UMAP analysis of synovial *CD45*$^+$ *CD11b*$^+$ *Ly6G*$^-$ monocyte-macrophages delineates the distribution of 18 subpopulations. (c) Pathway enrichment of DEGs revealed by KEGG. (d) Cell-specific enrichment of DEGs was determined in PaGenBase. (e) Immunohistochemistry of VSIg4 in the joints of healthy mice and mice undergoing knee medial meniscectomy (DMM) for 12 weeks. (f) HE and (g) Safranin O fast green staining, IHC for (h) C5b-9 and (i) C3, and (j) immunofluorescence staining for VSIg4 and CX3CR1 of SD rat joints 7 weeks after immunization with CFA in the footpad.

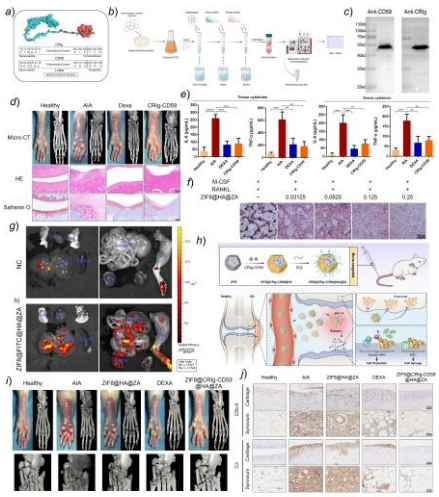

Figure 2. Anti-Rheumatoid Arthritis Activity of Dual-Targeting Nanoplatform. (a) Schematic diagram of CRIg-CD59 fusion protein design and mock protein structure. (b) The process of recombinant protein expression and purification in E. coli system. (c) Western-blotting detection of CRIg-CD59 recombinant protein. (d) Micro-CT, HE staining and safranin fast green staining of joints in AIA model. (e) Serum and tissue IL-6 and TNF-α protein levels. (f) Trap staining to detect osteoclastogenesis. (g) In vivo bone-targeting experiment. (h) Mechanism diagram of ZIF8@CRIg-CD59@HA@ZA treatment of AIA. (i) Representative hindpaw micro-CT images of AIA rat model. (j) Cartilage and synovial tissues were analyzed for C5b-9 and C3 by immunohistochemistry at the seventh week. Data are presented as mean ± SD (n = 3) and statistical analysis was performed using one-way ANOVA test by comparing to the control group. *p < 0.05, **p < 0.01 and ***p < 0.001; ns indicates no significant difference. The one-way ANOVA with the Tukey's multiple comparison test was used for statistical analysis.

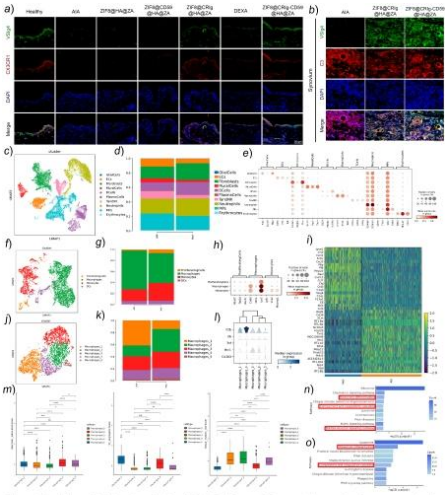

Figure 3. Regulation of the Macrophage Niche of RA by Dual-Targeted Therapy. (a) Immunohistofluorescence staining for VSIg4 and CX3CR1 in areas lining the synovium. (b) Immunohistofluorescence staining for VSIg4 and C3 in the synovium. (c) UMAP dimensionality reduction plot for unsupervised clustering of cell subtypes. (d) Percentage distribution of overall subclusters. (e) Dotplot of the top 3 cluster-specific marker genes. (f) UMAP dimensionality reduction plot for unsupervised clustering of MPs subtypes. (g) Percentage distribution of MPs subclusters. (h) Dotplot of the top 3 cluster-specific marker genes. (i) Heatmap of MPs overall differentially expressed genes. (j) UMAP dimensionality reduction plot for unsupervised clustering of Macrophages subtypes. (k) Percentage distribution of Macrophages subclusters. (l) Unsupervised clustering violin plot of M1 and M2 characteristic genes. (m) Functional evaluation gene set scores of macrophage subtypes; (n) KEGG enrichment of significantly downregulated DEGs in macrophages_1 subcluster. (o) KEGG enrichment of significantly downregulated DEGs in macrophages_4 subcluster.